SCIENTIFIC PAPER

ASSESSING INDOOR LEAD CORROSION USING RAMAN SPECTROSCOPY DURING ELECTROCHEMICAL REDUCTION

Marie-Claude Bernard[1], Virginia Costa[2], Suzanne Joiret[1]

1. Laboratoire Interfaces et Systèmes Electrochimiques, CNRS, UPR15-LISE, Université Pierre et Marie Curie-Paris 6, 4 Place Jussieu, 75005 Paris, France.

2. IRRAP- Institut de Restauration et de Recherches Archéologiques et Paléométallurgiques, 21 rue des Cordeliers, 60200 Compiegne, France

corresponding author:
suzanne.joiret@upmc.fr

Even though kept in cultural institutions, artefacts can be subjected to accelerated deterioration due to high concentration of pollutants in closed spaces. Potentially harmful conditions have been evaluated by electrochemical reduction of corrosion products formed on metallic coupons which have been exposed in selected places. In the case of silver coupons, this technique allowed chemical identification of the tarnish layer (sulphides and chlorides), as well as determination of the amount in which they are present on individual coupons. Extension of this approach to lead raises some difficulty as identification of the reduction peaks is more complex. In this work we combined electrochemical reduction of corrosion products with in-situ Raman spectroscopy to unambiguously correlate the reduction peaks with the compounds present on the surface of coupons previously exposed in different French institutions. Raman analysis carried out prior to the electrochemical reduction in a sodium sesquicarbonate solution revealed that the corrosion layer contains lead oxides, hydroxycarbonates and carbonates and in some cases formates and acetates.

1   Introduction

Lead reacts readily in natural atmospheres, forming a passive layer that will generally slow down further attack. However, in cases where organic acids are present, this protective layer can be transformed into soluble salts unable to protect the metal from further oxidation. These harmful compounds are not uncommon in museums and could come from diverse materials employed for storage and exposure of artefacts, like wood or glue. It is therefore very important to detect the presence of such compounds early enough to avoid irreversible damage to lead artefacts.

This work suggests the use of lead coupons as sensors, which, after reaction with the environment, will be analysed by Raman spectroscopy, XRD (x-ray diffraction analysis) and electrochemical reduc-

tion in order to characterize them qualitatively and quantitatively. This quantitative approach based on electrochemistry has already been successfully applied to silver by one of the author.[1,2]

2 Experimental

2.1 Exposure of the Metal Coupons

Lead coupons (commercial quality, Weber métaux) measuring 50 x 10 x 2 mm^3 have been mechanically prepared by grinding with a glass bristle just prior the exposure (counted in months) in the following locations:

A1   Angers Cathedral, vitrine Viollet-le-Duc - 18 months

BN1   Bibliothèque Nationale, cabinet de médailles, level A - 18 months

BN2   Bibliothèque Nationale, cabinet de médailles, level B - 18 months

PP1   Petit Palais, storage yellow - 24 months

PP2   Petit Palais, storage blue - 24 months

A typical setup for exposure is depicted in Figure 1, where the left image was taken at the Bibliothèque Nationale in Paris. The lead coupons were held in a plastic box insuring faces up and down exposure; together with lead, silver and cop-

Figure 1: Setup for the exposure; on the top - coupons exposed at the Bibliothèque Nationale, cabinet des médailles, Paris; on the bottom- lead before (a) and after exposure (b).

per coupons were also exposed for another purpose. The right image in Figure 1 depicts the differences in the aspect of the coupons before and after exposure.

2.2 Raman Spectroscopy and X-ray Diffraction Analysis (XRD)

The Raman spectrometer used for these studies is a HORIBA JobinYvon LABRAM consisting of an Olympus BX40 microscope confocally coupled to a 300 mm focal length spectrograph. The later is equipped with a holographic grating (1800 grooves/mm) and a Peltier cooled CCD detector (1024 × 256 pixels). The spectra were obtained with 632,817 nm radiation from an internal 10 mW HeNe laser with neutral density filters, 0.7 mW remaining at the sample, to avoid any thermal effects. For *ex-situ* measurements a 100× ULWD objective was used. For *in-situ* ones a 50× ULWD with a working distance of 8 mm allowed to record Raman spectra with a 5 mm thin electrolyte layer on top of the electrode.

X-ray diffraction analysis was carried out on each sample using a Philips diffractometer (Mo $K_{\alpha1}$ radiation) for 2 days exposure.

2.3 Electrochemistry

A classical three electrode electrochemical cell was used during this work. Reference electrode was a mercurous sulphate /saturated potassium sulphate electrode (V=0.650 V_{NHE}) to avoid any chloride leak from classical calomel electrode. A platinum grid could be applied as counter electrode. The sample surface of 0.2 cm^2 was delimited by a viton o-ring. Potentials and currents were imposed or measured with an EcoChemie potentiostat, voltammograms recorded at 5 mV/s. Chemicals for all solutions used in this work (sodium perchlorate pH 5.5, 0.1 M, borate buffer of pH 9.2 and sodium sesquicarbonate of pH 10, 0.1 M) are from Merck, Germany.

3 Results

3.1 Reference Spectra

Raman spectra for lead oxides and carbonates are well documented in the literature: PbO litharge and massicot,[3,4] $PbCO_3$ cerussite, $Pb_3(CO_3)_2(OH)_2$ hydrocerussite, $6PbCO_3.3Pb(OH)_2.PbO$ plumbonacrite.[5] However, since there is a lack of data regarding lead formate or lead acetate, reference spectra of these compounds have been recorded on a lead coupon previously exposed to
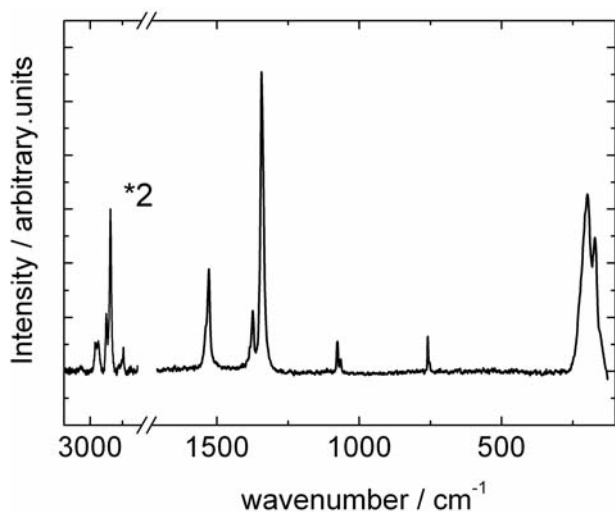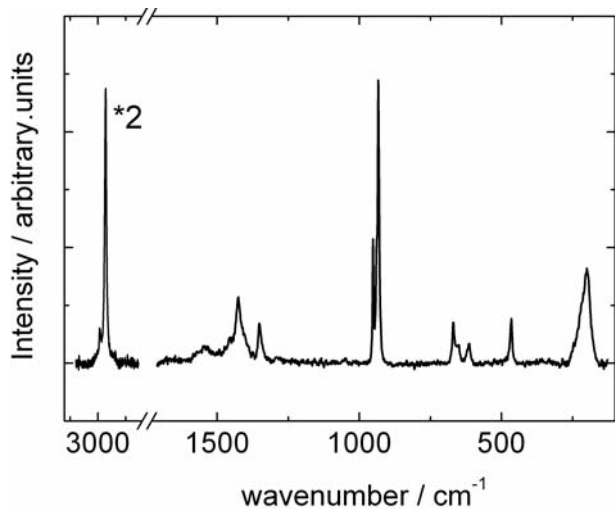
Figure 2: Raman spectrum of lead formate.

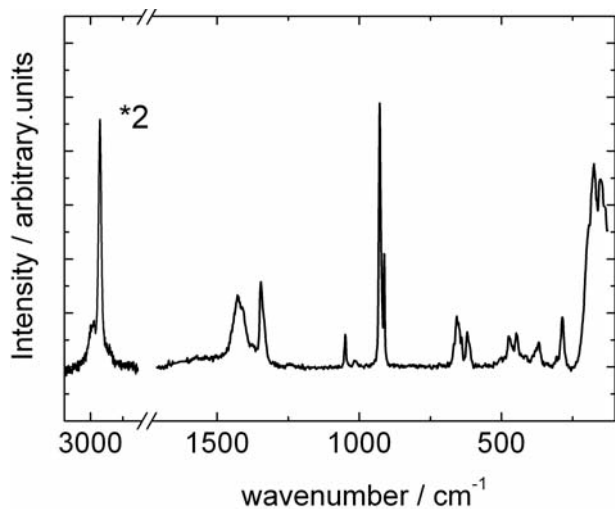Figure 3: Raman spectrum of lead acetate trihydrate.

Figure 4: Raman spectrum of basic lead acetate.

formic acid vapour and by using chemicals, respectively. In the case of formate, the resulting spectrum is shown in Figure 2, clearly presenting the main characteristic bands of such anion. Bands were assigned on the basis of the literature

on copper formate hydrates.[6,7] and are indexed in Table 1. There was no evidence of presence of any other lead(II) compound, like oxide or carbonate.

Regarding acetate, commercial lead acetate trihydrate and basic lead acetate (Alfa Aesar) were used and the recorded spectra are shown in the Figures 3 and 4, respectively. Bands assignments are given in Table 1, by comparison with well documented spectra of solid metallic acetates[8,9] and lead acetate complexes.[10] The main differences between the two spectra are the position of the doublet ν C-C at 930-950 cm^{-1} for the trihydrate and 910-930 cm^{-1} (as already stated but not shown by Black and Allen[11]) for the basic acetate and the presence of an extra band at 370 cm^{-1} (ν Pb-O in Pb-OH found at 404 cm^{-1} in $[Pb_4(OH)_4])^{4,12,13}$ for basic acetate. Lead formate is easily differentiated from lead acetates by the position of the C-H stretching bands, doublet centered at 2850 cm^{-1} for the formate and 2950 cm^{-1} for the acetates, the position of the C-O stretching band (1345 cm^{-1} for formate, 1414 cm^{-1} and 1407 cm^{-1} for acetates) and the absence of C-C stretching band in formate.

lead formate cm^{-1}	lead acetate trihydrate cm^{-1}	lead acetate basic cm^{-1}	assignment
173,2	198	177	Pb-O(org)
		286,37	Pb-OH
757	651,67	652, 657, 667	δ_s O-C-O
	930,95	910,93	ν C-C
		1050,11	ρ_{op} CH$_3$
1065,11	615	620,64	δ_{op} C-H / ρ_{op} O-C-O
	1346	1350	δ_s CH$_3$
1343	1414	1407	ν_s C-O
1374	466	447,47	δ_{ip} C-H / ρ_{ip} O-C-O
	1428	1430	δ'_{as} CH$_3$
1531,15		1515	ν'_{as} C-O
2844,29	2926,3	2930,3	ν_s, ν'_{as} C-H

Table 1: Band assignment for lead formate and lead acetates: ν - stretching (symmetric and anti-symmetric); δ - bending (symmetric and antisymmetric or in plane and out of plane); ρ - rocking (in plane and out of plane).

3.2   Ex-situ Raman and XRD Analysis

The results of ex-situ Raman and XRD analyses performed on the tarnished surface of coupons exposed in museums, were in agreement and are summarized in Table 2. There are no differences between face up and face down exposure.

Sample A1, exposed inside an oak cabinet in the Angers Cathedral, was covered with a very thick, white, quasi fluorescent layer of corrosion products (XRD analysis was unable to detect metallic lead on the contrary to the other coupons). The

sample	litharge α-PbO	massicot β-PbO	hydro-cerussite /cerussite	lead formate	lead acetate, basic
A1	-	-	x	x	x
BN1	x	-	x	x	x
BN2	X	-	X	-	x
PP1	x	x	-	-	-
PP2	X	-	X	X	x

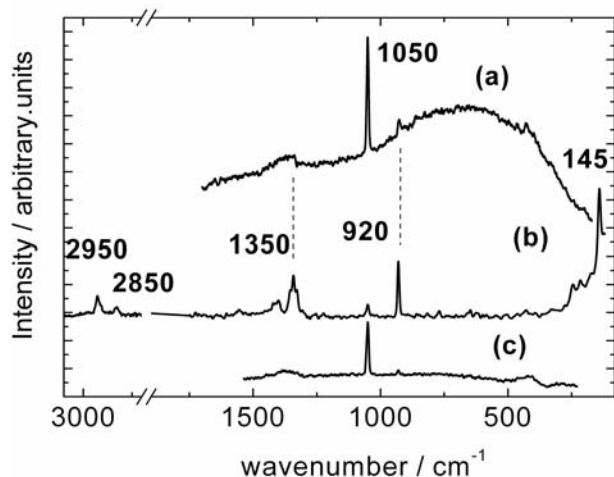Table 2: Corrosion products formed in the various samples.

Figure 5: Ex-situ Raman spectra of the samples A1 (a), PP2 (b) and BN1 (c).

typical Raman spectrum is the one of hydrocerussite with traces of basic acetate and formate, as stated by the presence of faint bands at 920 cm^{-1} and 1350 cm^{-1}, respectively, in Figure 5a. In the case of the coupons exposed in the Bibliothèque Nationale (BN1) stronger Raman bands of organics (920 cm^{-1} for basic acetate and 760 cm^{-1} for formate) are depicted in the spectrum with another compound, litharge (PbO) appearing with a strong band at 145 cm^{-1}. Furthermore, for BN1 sample hydrocerussite alone was found as a separated spectrum shown in Figure 5c, particularly on spots, where the corrosion layer is thicker. Sample BN2 presents less white spots on the surface than BN1 and shows no evidence of formate (spectrum not shown).

Analysis of coupons exposed in the Petit Palais put in evidence an important difference between the two environments chosen for the study: For the sample PP2, the most representative spectrum is a mixture of litharge (145 cm^{-1}), lead formate (2850 cm^{-1}), basic lead acetate (920 and 2950 cm^{-1}), cerussite and hydrocerussite (1055 and 1050 cm^{-1}, respectively), as depicted in Figure 5b. In this case, even though the relative peak intensities vary from place to place, those compounds were always found together; no spectrum presenting an isolated pure phase have been recorded.

On the surface of the specimen PP1 only litharge could be found (Figure 7a), but some spectra show also the presence of massicot with the typical band at 285 cm^{-1} in isolated places. The laser power was decreased to the minimum level as the thermal transformation of lead oxide is a well known process, but the characteristic bands of massicot were still appearing in the spectrum. Nevertheless, only lead(II) oxides are encountered on this sample.

These results are in accordance with the classical schematic process of atmospheric lead corrosion:[11] formation of a protective layer of lead(II) oxide (mainly litharge); CO_2 attack of the oxide layer according to:

$$2\ CO_2 + 3PbO + H_2O \rightarrow 2\ PbCO_3.Pb(OH)_2$$
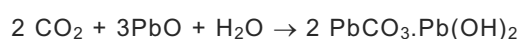
and in the presence of formic or/and acetic acid (C)OOH:

$$2\ HCOOH + PbO \rightarrow [Pb(HCOO)_2] + H_2O$$
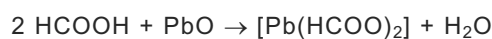
Those organic salts being further attacked by CO_2 are dissolved in water under the formation of lead carbonate and release of organic acid(s). This process results in a higher dissolution rate of lead with a thicker layer of corrosion products, as already stated by previous works.[14-16] On the thicker corrosion layers the end product is hydrocerussite.

3.3 Raman Spectroscopy During Electrochemical Reduction

Figure 6 presents the Raman spectra obtained for coupon BN1 (for PP2 or BN2 results are similar) under different conditions. Compared with the *ex-situ* result in Figure 6a, where the bands corresponding to organic compounds are shown, the *in-situ* spectrum in Figure 6b depicts the prompt dissolution of formate and acetate just after the immersion of the sample in the borate solution. The oxide band at 145 cm^{-1} still present at this open circuit condition (OCP) will disappear, when the sample is subsequently cathodically polarized at -1.3 V/SSE. The band of hydrocerussite at 1050 cm^{-1} remains in the spectrum even at lower potentials, as shown in Figure 6c. In the case of sample PP1, where only oxide was present at the beginning (Figure 7a), the same behaviour was observed and no corrosion products were left at -1.3 V/SSE, as shown in Figure 7b.

The polarization curves from open circuit potential to -1.3 V/SSE in buffered borate solution for the different samples are reported in Figure 8. It should be pointed out that the current peaks cor-
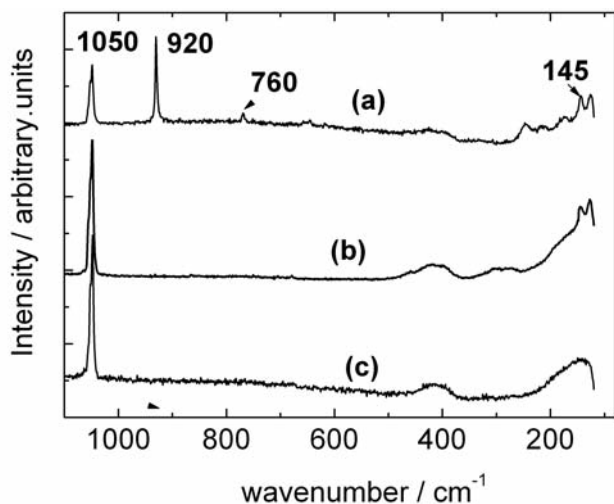
Figure 6: Raman spectra of the sample BN1. a) ex-situ; b) in borate solution at open circuit potential; c) in borate solution at -1.3 V/SSE.
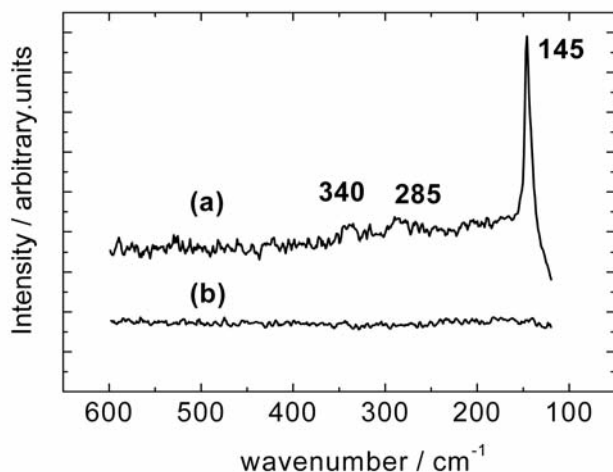

Figure 7: Raman spectra of sample PP1. a) ex-situ; b) in borate solution at -1.3 V/SSE.

respond to the reduction of lead oxide into metallic lead,[17] which is fully in agreement with the results obtained by Raman spectroscopy. The electrochemical tests were performed at the centimetric level (0.2 cm^2 of active surface) - three times for each coupons. The results are highly reproducible despite the inhomogeneity of the sample surfaces pointed out by Raman spectroscopy at the micrometric level.

Hydrocerussite could not be completely reduced in the different tested solutions even in more acidic sodium perchlorate, since at the applied potential range oxygen reduction is taking place simultaneously, increasing the local pH and stabilizing the basic carbonate. Furthermore, in the case of sample A1, the corrosion layer was so thick due to the harmfulness of the environment that it could not be electrochemically reduced. In such cases, it is necessary to shorten the exposure time.
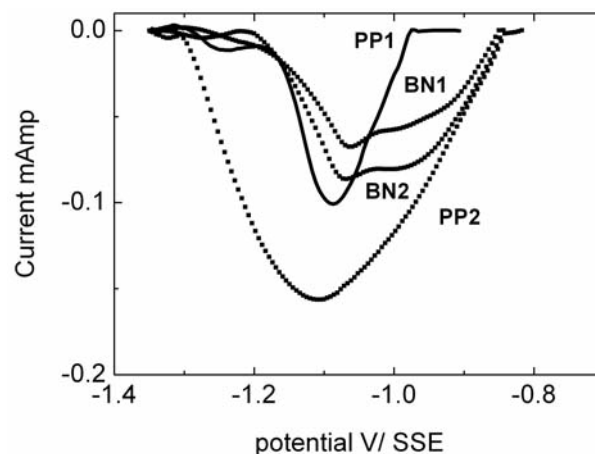

Figure 8: Current versus potential (voltammogram) at 5 mV/sec in borate solution for PP1, PP2, BN1 and BN2 coupons.

sample	corrosion rate (nm PbO/year)
A1	-
BN1	1.2
BN2	1.1
PP1	0.36
PP2	2.4

Table 3: Corrosion rate (nm/year) of the various specimen.

The charge involved in the reduction reaction was obtained through integration of the area under the corresponding peak in the polarization curves. Assuming that the corrosion layer is constituted by PbO (density 9.53 g/cm^3), it is possible to evaluate its equivalent thickness, which, divided by the exposure period, gives the corrosion rate.

Table 3 reports such rates for the tested samples. It is worth to notice the difference in the corrosivity (regarding lead) presented by two locations in the same institution: While the rates calculated for the two samples in the Bibliothèque Nationale are not very far apart, in the case of the Petit Palais the sample PP2 reacts almost 2 times faster than the other coupons. The higher corrosion rate of specimen PP2 is supported by the stronger intensity of the Raman bands for formate, acetate and litharge compared with the one of hydrocerussite, which points out larger amount of organic pollutants for PP2 than for the other locations.

4   Conclusion

The combination of Raman spectroscopy and electrochemistry allows a qualitative and quantitative evaluation of the environmental impact on the corrosion of lead. Measurements performed on lead sensors exposed for short periods reveal remarkable differences between different rooms in the

same institution. Moreover, the relative amount of organic salts detected in the corrosion products was particularly high for the most corroded sample. Further work is in progress aiming to improve the method in order to be able to reduce the carbonate layer, and in this way, evaluate its thickness.

5   References

1. V. Costa, *Electrochemical techniques applied to metals conservation,* Materials Research Society Symposium Proceedings, 2005, **852**, 89-96.

2. V. Costa, D. David, P. Dillmann, L. Robbiola, *Paleocorrosion, an imprint of the past,* Revue de Metallurgie/Cahiers d'Informations Techniques, 2002, **99**, 751-760.

3. H. G. M. Edwards, E. L. Dixon, I. J. Scowen, F. R. Perez, *Lead-tin mirror formation from mixtures of red lead and tin sulphide,* Spectrochim. Acta, 2003, **59A**, 2291-2299.

4. L. Burgio, R. J. H. Clark, S. Firth, *Raman spectroscopy as a means for the identification of plattnerite (PbO$_2$), of lead pigments and of their degradation products,* Analyst, 2001, **126**, 222-227.

5. M. H. Brooker, S. Sunder, P. Taylor, V. J. Lopata, *Infrared and Raman spectra and x-ray diffraction studies of solid lead(II) carbonates,* Can. J. Chem., 1983, **61**, 494-502.

6. A. M. Heyns, *Vibrational spectra of the copper(II) formates. I. Raman spectra of polycrystalline copper(II) formate tetrahydrate and the light blue modification of anhydrous copper(II) formate,* J. Mol. Struct., 1973, **18**, 471-485.

7. R. O. Carter, B. D. Poindexter, W. H.Weber, *Vibrational spectra of copper formate tetrahydrate, copper formate dihydrate and three anhydrous forms of copper formate,* Vibr. Spectrosc., 1991, **2**, 125-134.

8. A. W. Musumeci, R. L. Frost, E. R. Waclawik, *A spectroscopic study of the mineral paceite (calcium acetate),* Spectrochim. Acta, 2007, **67A**, 649-661.

9. R. L. Frost, J. T. Kloprogge, *Raman spectroscopy of the acetates of sodium, potassium and magnesium at liquid nitrogen temperature,* J. Mol. Struct., 2000, **526,** 131-141.

10. M. M. Yang, D. A. Crerar, D. E. Irish, *A Raman spectroscopic study of lead and zinc acetate complexes in hydrothermal solutions,* Geochim. Cosmochim. Acta, 1989, **53**, 319-326.

11. G. C. Allen, L. Black, *Role of organic acids in lead patination,* Brit. Corr. J., 2000, **35**, 39-42.

12. S. M. Grimes, S. R. Johnston, I. Abrahams, *Characterization of the predominant low-pH lead(II)hydroxo cation, [Pb$_4$(OH)$_4$]$^{4+}$; crystal structure of [Pb$_4$(OH)$_4$][NO$_3$]$_4$ and the implications of basic salt formation on the transport of lead in the aqueous environment,* J. Chem. Soc., Dalton, 1995, **12**, 2081-2086.

13. J. O. Jensen, *Vibrational frequencies and structural determinations of Pb$_6$O(OH)$_6$$^{4+}$,* THEOCHEM, 2003, **635,** 11-24.

14. A. Niklasson, L. G. Johansson, J. E. Svensson, *Atmospheric corrosion of lead. The influence of formic acid and acetic acid vapors,* J. Electrochem. Soc., 2007, **154**, C618-625.

15. A. Niklasson, L. G. Johansson, J. E. Svensson, *Influence of acetic acid vapor on the atmospheric corrosion of lead,* J. Electrochem. Soc., 2005, **152**, B519-B525.

16. J. Tetreault, E. Cano, M. van Bommel, D. Scott, M. Dennis, M. G. Barthes-Labrousse, L. Minel, L. Robbiola, *Corrosion of copper and lead by formaldehyde, formic and acetic acid vapors,* Stud. Cons., 2003, **48**, 237-250.

17. B. Schotte, A. Adriaens, F. Dhooghe, D. Depla, M. Dierick, M. Dowsett, E. Lehmann, P. Vontobel, *Chemical and morphological changes of historical lead objects as a result of the use of electrolytic reduction as a stabilization treatment,* Anal. Chem., 2006, **78**, 8319-8323.